

Original Article

FDTD Analysis of Union-Shaped Triple Band Microstrip Patch Antenna using the Novel Algorithm for Identification of Contiguous White Pixels in a Column of an Image

Girish Bhide¹, Anil Nandgaonkar², Sanjay Nalbalwar³, Brijesh Iyer⁴

^{1,2,3,4}Dr. Babasaheb Ambedkar Technological University, Lonere, Maharashtra, India

¹Corresponding Author : ggb_rtm@yahoo.co.in

Received: 25 July 2022

Revised: 22 September 2022

Accepted: 07 November 2022

Published: 24 December 2022

Abstract - This article proposes a union-shaped triple band microstrip patch antenna design suitable for WLAN and wireless sensor applications. The union shape is obtained by optimizing the combination of a rectangular shape and two semicircles. It is designed using an FR-4 substrate having a dielectric constant of 4.4. The antenna size is 34.6 mm × 48.4 mm × 1.6 mm. It exhibits three resonance frequencies such as 2.4 GHz, 4.8 GHz, and 6.8 GHz. The S_{11} values at these frequencies are -23dB, -20 dB, and -21 dB, respectively. The FDTD analysis of this proposed antenna is carried out with a novel algorithm developed for identifying strips of contiguous white pixels in a column within a black-and-white image of the antenna. The algorithm reads all the pixels in the black and white image and forms separate strips having white color, indicating the conducting part of the antenna. The data of all the strips are stored in one structure containing several fields such as strip number, column number in which the strip is present, the starting row number, the last row number, and the total length of the strip. This structure was then used to create the antenna's geometry in the FDTD environment using Elsherbini codes. This algorithm will stand as a better solution for implementing the geometry of microstrip patch antennas for carrying out FDTD analysis.

Keywords - Union shaped, Triple band antenna, FDTD analysis, Strip identification algorithm, WLAN, and wireless sensor.

1. Introduction

Microstrip patch antennas (MSAs) are widely used for various wireless communication applications such as space communication, cellular communication, wireless LAN, WiMAX, etc. It is because they offer advantages like low profile, low weight, inexpensive, easily integrable with electronic components, etc. These antennas are also suitable candidates for dual-band and triple-band operations.

A triple-band rectangular slot MSA suitable for wireless applications is discussed in [1]. Two slits and T-shaped slots are used to get a triple band performance for WLAN, Bluetooth, and 5.8 GHz/ISM Band applications, as explained in [2]. A bus-shaped tri-band antenna performing 5G applications in the sub-6 GHz band is reported in [3]. A triple band printed monopole antenna appropriate in wireless applications and its uniaxial PML-FDTD analysis is given in [4]. A compact flower-shaped direct-fed hexagonal MSA with triple band-notch is reported in [5]. A CPW-fed monopole triple-band antenna designed using the FDTD method is discussed in [6]. A triple-band MSA for wireless LAN applications is reported in [29]. A tri-band antenna using L-shaped slots suitable for BT/WLAN/WiMAX applications is discussed in [8].

An MSA using an inverted F-slot providing triple-band performance suitable for the WiMAX application is explained in [9]. A triple-band antenna design using a square ring technique is presented in [10]. A metamaterial-inspired triple band antenna is reported in [11]. A triple-band performance obtained using an E-shaped antenna is discussed in [12]. A fork-shaped compact triple-band antenna is reported in [13]. A microstrip patch antenna designed using a U slot for exhibiting triple band performance is discussed in [14]. A W-shaped microstrip antenna providing three resonance bands is discussed in [15].

In this article, the design of a union-shaped triple-band MSA is discussed. It is based on the previous work of dual band high gain MSA [30]. In this, some part of the rectangular microstrip patch is replaced by two semicircles, forming a union shape. L-shaped slots are now included over the union shape, giving triple-band performance. Many articles present the full-wave analysis of MSAs using the FDTD method [17-20]. However, these articles neither reveal the details of filling material index over the FDTD grid nor suggest simple and effective techniques. The application of image algorithms for filling material index is the new trend presented in [21].



Successful implementation of this trend is demonstrated in [22]. However, this trend has a minor issue: the need to manually decide the values of circle radius, center coordinates, coordinates of triangle vertices, etc.

In this work, a novel algorithm for analyzing a binary image for extracting a contiguous strip of white pixels is developed and then used to put the material index in the FDTD investigation of the planned triple band MSA. It dramatically reduces manual work, as found in [21-22].

2. Antenna Design

The antenna's shape is developed with the objective of a triple-band outcome. Initially, a rectangular antenna based on standard formulae was designed using an FR-4 substrate having a dielectric constant of 4.4 and a height of 1.6 mm [23]. It was designed initially at a nominal frequency of 2.5 GHz. The patch length and width are 28.2 mm and 36.5 mm, severally. The final antenna was designed iteratively, which is explained here. In the first iteration, the patch length is unchanged, while the width is reduced to 28 mm. The reduced width is compensated by adding two semicircles, each of a 9 mm radius, to keep the patch area almost the same as that of the nominal design with a 2.5 GHz frequency. A skew symmetry is used to arrange the semicircles. Fig. 1 presents the antenna sketch in iteration 1.

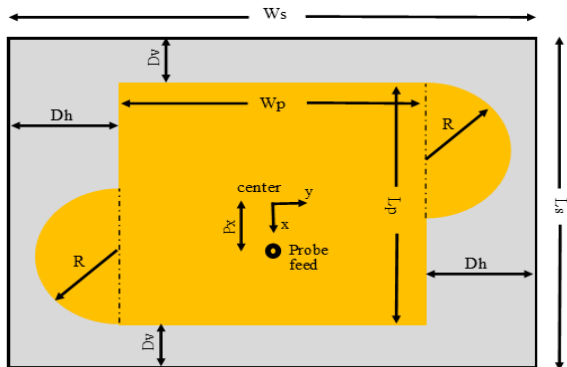


Fig. 1 Sketch of Iteration 1

In iteration 2, the vertical slots near the width edges, i.e., parallel to the length, are used. The slot length after optimization was set to 18.3mm. Fig. 2 shows the antenna sketch in iteration 2.

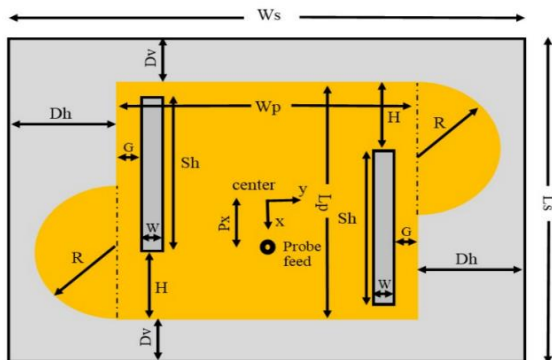


Fig. 2 Sketch of Iteration 2

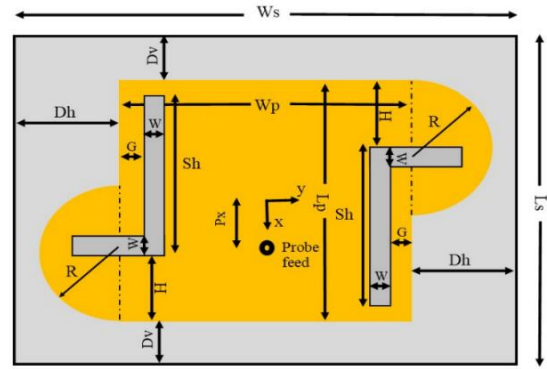


Fig. 3 Sketch of Iteration 3 - proposed antenna

Iteration 3, i.e., the planned antenna, is formed by adding horizontal slots perpendicular to vertical slots. The horizontal slots extend midway through the semicircles. This is the proposed union-shaped antenna as presented in fig. 3. The L shape slots of 1.3 mm width are positioned near the width edges, i.e., parallel to the length and through the center line of the semicircular shapes. The slot lengths were optimized to get the desired triple-band performance. The antenna has a complete ground plane and a co-axial probe feeding along the vertical center line. The black and white images of these iterations were supplied to the proposed novel algorithm of strip identification.

The algorithm generates the strip number, the column number, starting row number, the end row number, and the length of the white strip. This algorithm output places the material index over the FDTD mesh. Section III discusses the algorithm, and table 1 represents the optimized dimensions of the antenna.

Table 1. Proposed Antenna Dimensions

Label	Length (mm)	Label	Length (mm)	Label	Length (mm)
Ls	34.6	R	9.0	Dh	12.2
Ws	48.4	Sh	18.3	Dv	3.2
Lp	28.2	Sw	6.7	H	8.4
Wp	24.0	Px	5.5	G	1.0
W	1.3	-	-	-	-

3. Strip Identification Algorithm

When the FDTD method is used to get the performance outcome of an MSA, the completion of various tasks is necessary. Some of these are discretization in the spatial domain, i.e. deciding values of dx, dy, and dz, selecting the boundary condition, deciding the number of iterations, assigning the material indices, etc. [24-26]. However, placing material indexes over the FDTD mesh out of these is always challenging, especially when the shape is irregular. It was thought to develop a novel algorithm that would simplify this job by accepting a black-and-white image of the antenna and then extracting the contiguous white pixels representing the conducting material (patch) of the antenna. The algorithm relies on reading the pixels in a column to find out the vertical

strips of contiguous white strips. It is important to note that when a new white pixel is found, the decision has to be taken whether it can be connected with the ongoing strip or a new strip is to be initiated. Further, the ongoing strip needs to be terminated when a column ends.

The motivation for the development of the algorithm lies in the similarity between a 2D image of an object and an index-filled FDTD mesh. In the case of an image, the light intensity values are stored for all the pixels in the image. In contrast, in the case of index-filled FDTD mesh, for every node, the number representing either conducting material or dielectric material is stored. The algorithm is an outcome of an inspiration based on the concept of run-length encoding of an image [27-28]. The algorithm proposed in this work employs a data structure consisting

of five fields: number, col_num, starting_row, end_row, and length. Here, the number means the strip number, and col_num is the column of the black-and-white image in which this strip is found, representing the 'y' coordinate. Further, the starting_row and end_row are the strip's limits in the 'x' direction. Table 2 presents the novel strip identification algorithm.

The algorithm is set up by writing MATLAB code. The yield of the MATLAB code, i.e., the structure containing values of the corresponding column number in which the brick is found in the image, starting row number, end row number, etc., is used to create the bricks in the FDTD environment. Fig. 4 shows a flowchart that nicely explains the algorithm.

Table 2. The Novel Strip Identification Algorithm

```

Read the binary image
  Find out the number of rows and columns
  Initialize various supporting variables as given below.
[old_strip = 0, starting_row = 0, strip_old = 0, m = 0, n = 1]
For all j Do ...{j indicates image column number}
  For all i Do ...{i indicates image row number}
    Is the pixel White
      if yes check is strip_old = 0{begin new strip}
        if yes fill the fields of data structure of the strip
          increment index i.e. m = m + 1
          [strip(m).number = oldstrip + 1, strip(m).col_num = j]
          [strip(m).starting_row = i, strip(m).end_row = i]
          [strip(m).length = 1]
          n = strip(m).starting_row ...{remember the starting row}
          oldstrip = strip(m).number ...{remember the strip number}
          strip_old = 1 ...{strip is going on}

          else if check is strip_old = 1{is there ongoing strip}
            if yes fill the fields of data structure of the strip
              [strip(m).number = oldstrip, strip(m).col_num = j]
              [strip(m).starting_row = n, strip(m).end_row = i]
              [strip(m).length = i - n + 1]
              [starting_row = i]
            end
          end
        Is the pixel Black
          strip_old = 0
        end
      strip_old = 0
    end
  ... {structure for the creation of white strips is over}
  display the total number of strips ...{current value of m}
  Using the data written in the above structure ["strip"]
Find and display the smallest and largest values of the following.
[column number, starting row number, end row number, length]
----- End of the Algorithm -----

```

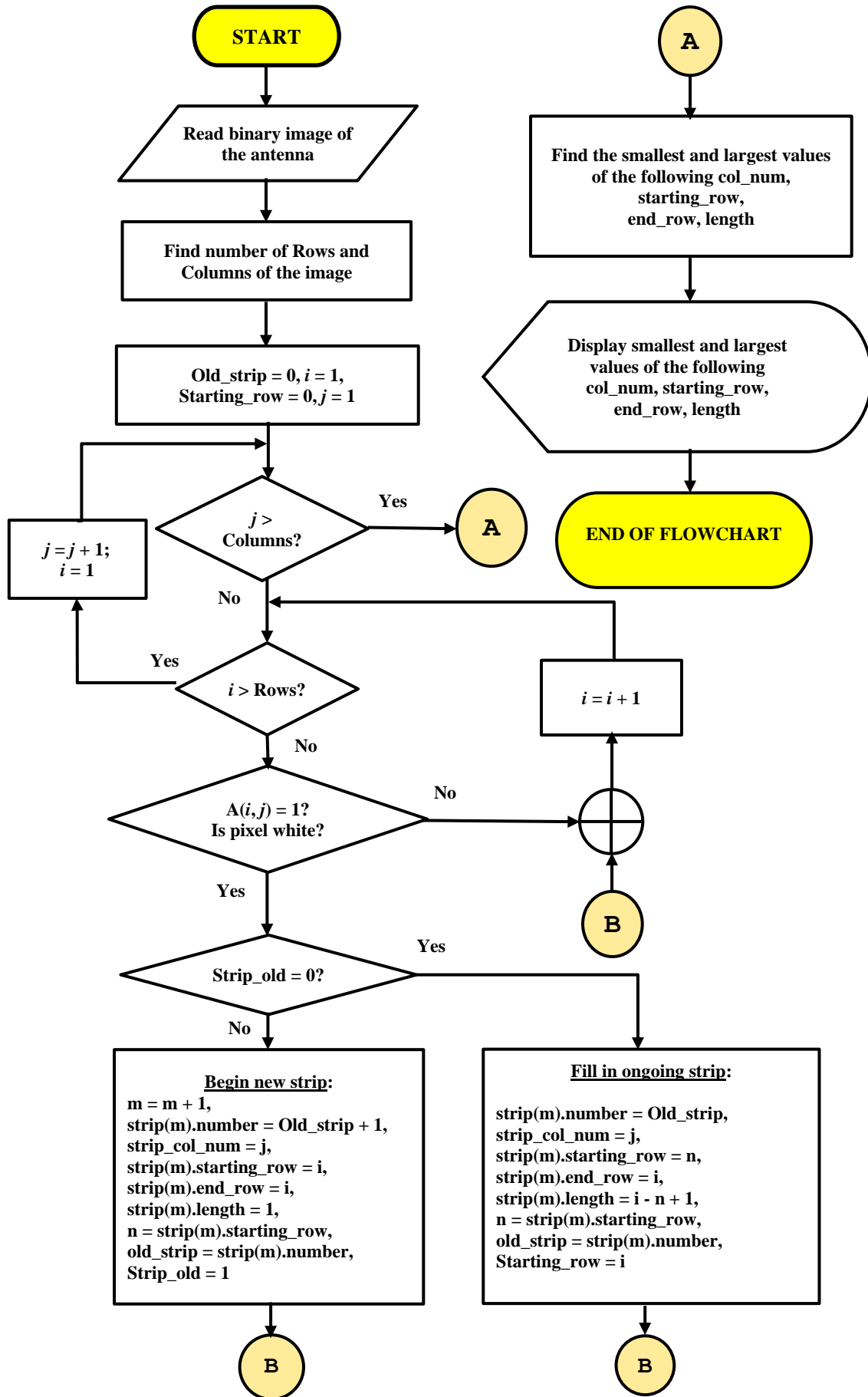


Fig. 4 Flowchart of Strip Identification Algorithm

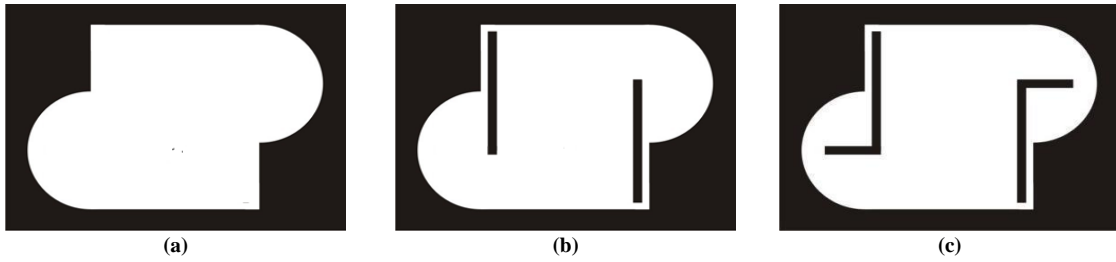


Fig. 5 Images of the three iterations of antenna fed to the algorithm a) Iteration1 b) Iteration2 c) Iteration 3

Table 3. Output of Algorithm

Parameters of White strips	Iteration 1		Iteration 2		Iteration 3	
	Value	Explanation	Value	Explanation	Value	Explanation
total number of strips	420	$10*(W_p + 2R)$ (64 columns have no White pixel at all)	446	$10*(W_p + 2R + 2*(1.3))$ (each 1.3 mm wide slot uses 13 columns)	600	$10*(W_p + 2R + 2*9)$ (The width of L shape slot in the horizontal direction is 9 mm)
smallest column number	33	$(10*(D_h - R) + 1)$ i.e. column of leftmost strip	33	$(10*(D_h - R) + 1)$ i.e. column of leftmost strip	33	$(10*(D_h - R) + 1)$ i.e. column of leftmost strip
largest column number	452	$484 - (10*(D_h - R))$ i.e. column of rightmost strip	452	$484 - (10*(D_h - R))$ i.e. column of rightmost strip	452	$484 - (10*(D_h - R))$ i.e. column of rightmost strip
smallest starting row number	33	$10*D_v + 1$ i.e. top border of the patch	33	$10*D_v + 1$ i.e. top border of the patch	33	$10*D_v + 1$ i.e. top border of the patch
largest starting row number	210	Leftmost strip	305	$10*(34.6 - D_v - 1) + 1$	305	$10*(34.6 - D_v - 1) + 1$
smallest end row number	130	Rightmost strip	42	Small space = 1 mm in the top edge of conducting patch and vertical slot.	42	Small space = 1 mm in the top edge of conducting patch and vertical slot.
largest end row number	314	$10*(L_s - D_v)$	314	$10*(L_s - D_v)$	314	$10*(L_s - D_v)$

3.1. Implementation of the Algorithm

A MATLAB code is developed for the implementation of the algorithm. The algorithm extracts the white pixel strips representing the conducting part of the antenna based on the black-and-white image input. The black-and-white image of every iteration is inputted into the code. Fig. 5 shows all three images of the three iterations. Table 3 shows the output given by the MATLAB code.

4. FDTD Analysis

The FDTD performance outcome of MSA involves the selection of boundary conditions such as UPML, CPML, or any other, further deciding spatial discretization, field update equations, update coefficients, time looping, using suitable source and the feed model, etc. Many papers discuss these aspects [17-20]. One of the critical tasks in FDTD implementation is filling the material index over the FDTD grid, i.e. correct realization of the antenna's geometry. A detailed explanation of filling the material index is found in [21].

4.1. FDTD Setup

The substrate dimension is 34.6 mm x 48.4 mm x 1.6 mm. The dx, dy, and dz (spatial discretization) are 0.1mm, 0.1mm and 0.4mm, respectively. Eq. (1) shows the formula for the calculation of the number of cells in the "x" direction, which is called "nx". The values of "nx", "ny", and "nz" is given by eq. (2 – 4) serially. A co-axial probe feeds this antenna at 5.5 mm away from the center along the vertical line of symmetry.

$$nx = \frac{\text{length in x direction}}{dx} + 2(\text{CPMLbuffercells} + \text{Airbuffercells}) \quad (1)$$

$$nx = \frac{48.4 \text{ mm}}{0.1 \text{ mm}} + 2(8 + 10) = 520 \quad (2)$$

$$ny = \frac{34.6 \text{ mm}}{0.1 \text{ mm}} + 2(8 + 10) = 382 \quad (3)$$

$$nz = \frac{1.6 \text{ mm}}{0.4 \text{ mm}} + 2(8 + 10) = 40 \quad (4)$$

The data structure filled in after the execution of MATLAB code based on the algorithm of this work contains the data to create the geometry. The routine "define geometry" from the well-known resource (Book by Atef Elsherbeni) is used [25]. Fig. 6 shows the developed geometry in the FDTD environment.

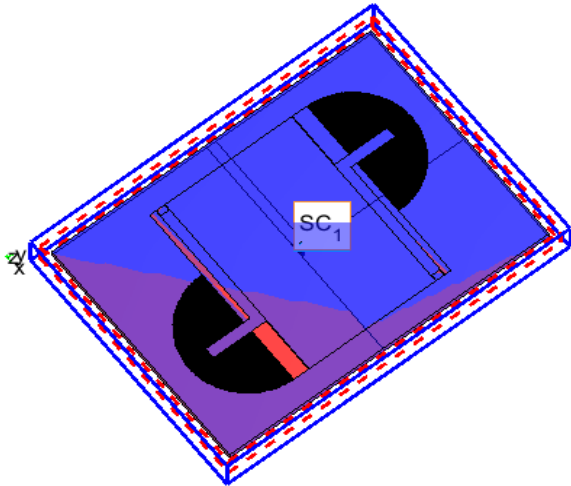


Fig. 6 The geometry of the antenna developed in the FDTD environment

Table 4 shows the FDTD arrangement ("setup") to execute the FDTD simulation codes in the MATLAB environment.

Table 4. FDTD Setup

Parameter	Value	Parameter	Value
nx	520	Dx (in mm)	0.1
ny	382	dy (in mm)	0.1
nz	40	dz (in mm)	0.4
CPML cells (buffer)	8	time steps	5000
Air cells (buffer)	10	Caurant's factor	0.9

Fig. 7 shows the return loss S_{11} obtained from the FDTD simulation for all three iterations.

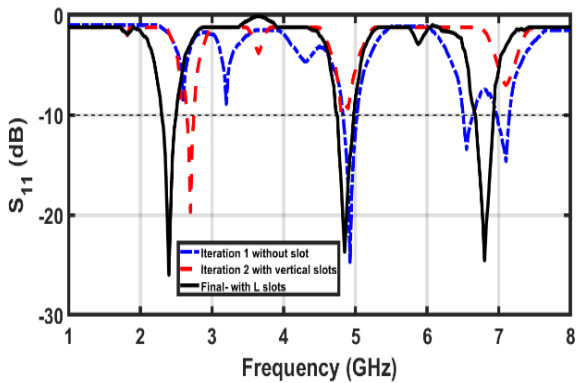


Fig. 7 Simulated S_{11} Results

5. Results and Discussions

Fig. 8 depicts the fabricated model of the union-shaped antenna. The substrate dimensions are 34.6 mm x 48.4 mm x 1.6 mm.

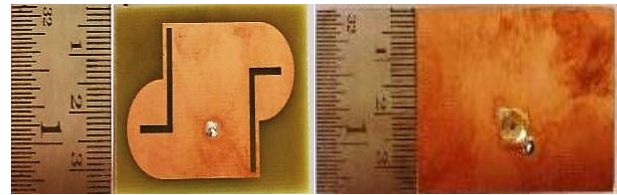


Fig. 8 Fabricated model of antenna a) Top patch b) ground plane

The antenna performance parameters were measured with the help of a Vector network analyzer from Rohde & Schwarz ("2 ports, 13.6 GHz, model ZVL13"). Fig. 9 shows the comparison of measured S_{11} values with values obtained through simulation. It is seen that the measured values of S_{11} are almost matching with FDTD analysis. The -10 dB bandwidths obtained are from 2.35 GHz to 2.5 GHz, i.e. (6.18%), 4.75 GHz to 4.95 GHz, i.e. (4.12%), and 6.7 GHz to 6.95 GHz, i.e. (3.66%).

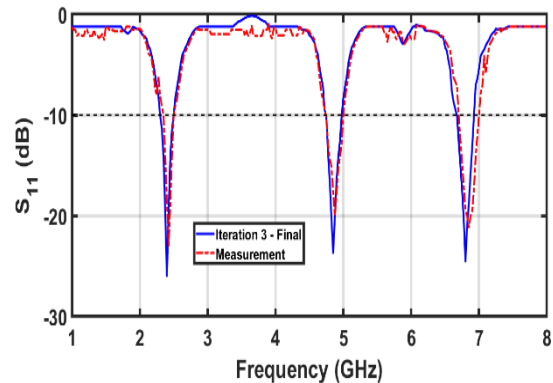


Fig. 9 Comparison of S_{11} of iteration 3 - Simulation vs measurement.

Table 5 compares the proposed antenna's measured gain with the simulated gain.

Table 5. Gain Comparison

Sr.	Freq (GHz)	Gain Simulated (dBi)	Gain Measured (dBi)
1	2.4	4.75	5.98
2	4.8	5.27	6.67
3	6.8	5.96	5.07

It is found that both the gains measured and simulated are very nearby to the total bandwidth. This antenna's radiation patterns are measured in XZ and YZ planes. The frequencies used for measurement are 2.4 GHz, 4.8 GHz, and 6.8 GHz. These radiation patterns are observed to be steady at all three frequency ranges. These measured and simulated patterns of radiation are depicted in fig. 10, 11, and 12 serially. The measured radiation patterns are in good agreement with the simulated ones.

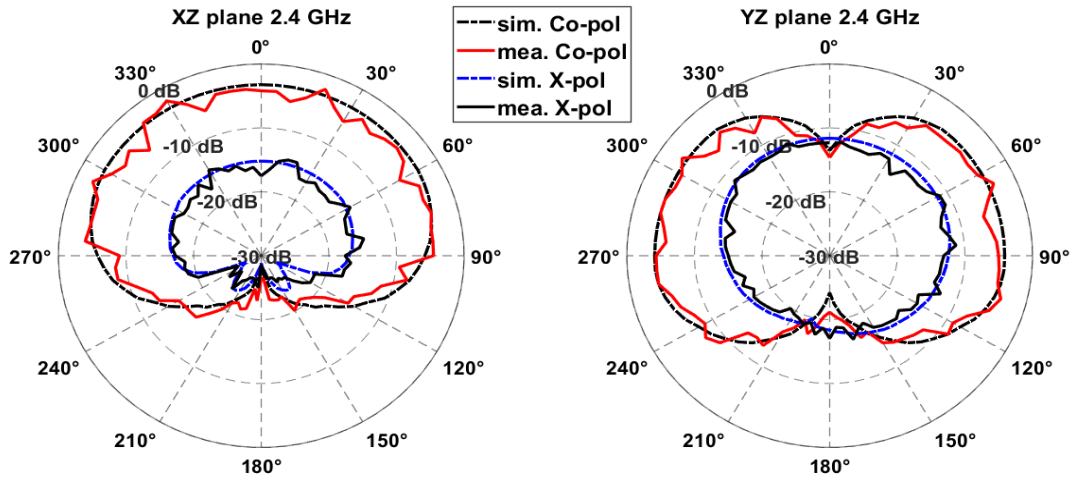


Fig. 10 Radiation Patterns at 2.4 GHz - Measured and simulated

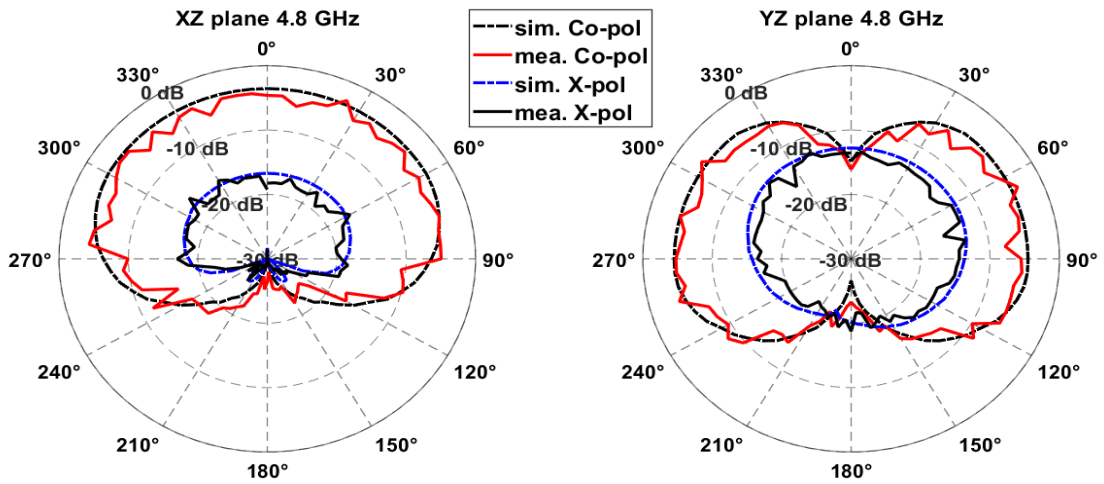


Fig. 11 Radiation Patterns at 4.8 GHz - Measured and simulated

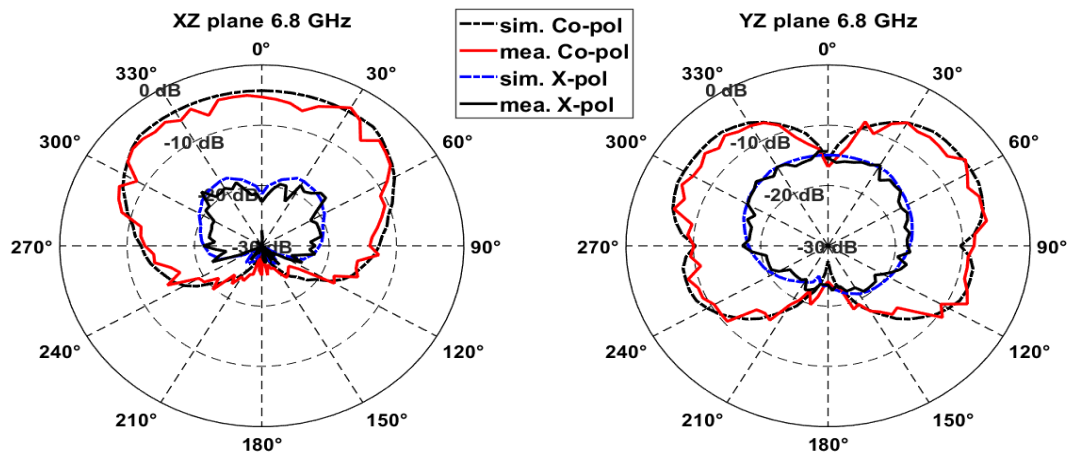


Fig. 12 Radiation Patterns at 6.8 GHz - Measured and simulated

Table 6. Comparison of Proposed Union-Shaped Triple Bands Antenna with other Triple Band Antennas

Reference No.	Frequency Bands (GHz)	Gain (dBi) Minimum - Maximum	Substrate name and its height	Area of Patch (mm ²)	Technique employed
[1]	2.4, 5.5, 7.5	1.24 - 3.57	FR4, 1.6 mm	53 x 53	Rectangular slot
[6]	2.4, 5.2, 5.8	Not given	FR4, 1.6 mm	63 x 57.6	CPW fed planar monopole
[9]	2.4, 3.9, 5.7	5.77 - 7.74	RT 5880 3.175 mm	67 x 74	Inverted F slot
[14]	5.59, 6.1, 6.8	5.5 – 8.00	FR4, 1.99 mm	56 x 50	U slot
Proposed	2.4, 4.8, 6.8	4.75 – 6.67	FR4, 1.6 mm	34.6 x 48.4	Union shape with L slots

Table 6 shows the qualitative comparison of the proposed antenna with similarly reported models. The complexity in the design of similarly reported models is higher than the proposed antenna. The proposed antenna is tiny in size compared to the cited references. The proposed antenna has more steady radiation patterns over all three bands. The development of a novel strip identification algorithm for obtaining FDTD performance outcomes is a crucial component of the work mentioned in this article.

6. Conclusion

A union-shaped triple band MSA is developed to perform in frequency bands suitable for WLAN application. It is analyzed using the novel strip identification algorithm. The antenna model is fabricated using an FR-4 substrate. The size of MSA is 34.6 mm x 48.4 mm x 1.6 mm. The proposed antenna offers an S_{11} below -15 dB (less than) over the three bands of 2.35 to 2.5 GHz, 4.7 to 4.9 GHz, and 6.6 to 7.1 GHz. The maximum gain of this antenna changes from 4.75 dBi to 6.67 dBi over the three bands. The proposed antenna model is appropriate for WLAN applications and wireless sensor networks.

References

- [1] M. B. Hossain, and M. F. Hossain, "Design of a Triple Band Rectangular Slot Microstrip Patch Antenna for Wireless Applications," *2020 IEEE Region 10 Symposium (TENSYP)*' 2020, pp. 1832-1835, 2020. *Crossref*, <http://dx.doi.org/10.1109/TENSYP50017.2020.9230997>
- [2] K. Mondal, P.P. Sarkar, and D. C. Sarkar, "High Gain Triple Band Microstrip Patch Antenna for WLAN, Bluetooth, and 5.8 GHz/ISM Band Applications," *Wireless Personal Communication*, vol. 109, pp. 2121–2131, 2019. *Crossref*, <https://doi.org/10.1007/s11277-019-06671-w>
- [3] A. Kamran et al., "A Bus Shaped Tri-Band Antenna for Sub-6 GHz 5g Wireless Communication on Flexible PET Substrate," *2019 22nd International Multitopic Conference (INMIC)*, pp. 1-6, 2019. *Crossref*, <https://doi.org/10.1109/INMIC48123.2019.9022764>
- [4] H. K. Bora, E. Gogoi, and Dipak Kr. Neog, "UPML-FDTD Analysis of Triple Band Monopole Antenna for Wireless Applications," *International Journal of Electronics Engineering Research Propagation*, vol. 9, no. 5, pp. 649-654, 2017.
- [5] Sayed Arif Ali, D. Jhanwar, and D. Mathur, "Design of a Compact Triple Band-Notch Flower-Shaped Hexagonal Microstrip Patch Antenna," *2016 International Conference on Information Technology INCITE'2016*, pp. 293-298, 2016. *Crossref*, <https://doi.org/10.1109/Incite.2016.7857634>.
- [6] Zengrui Li et al., "Design of Triple-Band CPW-Fed Planar Monopole Antenna Using FDTD Method," *2010 International Conference on Microwave and Millimeter Wave Technology, ICMMT'2010*, pp. 953-956, 2010. *Crossref*, <https://doi.org/10.1109/ICMMT.2010.5525140>
- [7] Kuang Fuqiang et al., "A Triple-Band Microstrip Antenna for WLAN Applications," *2010 International Conference on Communications and Mobile Computing, ICCMC'2010*, pp. 68-71, 2010. *Crossref*, <https://doi.org/10.1109/CMC.2010.66>

The performance of the novel Strip identification algorithm is highly accurate and suitable for antennas having any irregular shape. It will stand as an ultimate solution for implementing geometry in the FDTD analysis.

In the future, this newly developed algorithm can be improved to merge the strips having the same starting row number and the same end row number in adjacent columns. It will reduce the number of bricks created in the FDTD environment. There is much scope to further improve the union shape design by splitting each semicircle into two semicircles having unequal radii.

Acknowledgement

The authors hereby acknowledge the cooperation offered by Mrs. Leena Bhamare, of Circuit Vision, for fabrication work. The authors also thank Dr. Anand Kakade and Mr. Vijay Patil of the Rajarambapu Institute of Technology, Rajaramnagar, Maharashtra, for testing the antenna model.

- [8] N. Mahmoud, and E. K. I. Hamad, "Tri-Band Microstrip Antenna With L-Shaped Slots for Bluetooth/WLAN/WIMAX Applications," *2016 33rd National Radio Science Conference NRSC'2016*, pp. 73-80, 2016. *Crossref*, <https://doi.org/10.1109/NRSC.2016.7450826>
- [9] S. Panusa, and M. Kumar, "Triple-Band Inverted F-Slot Microstrip Patch Antenna for WIMAX Application," *2014 International Conference on Medical Imaging M-Health and Emerging Communication Systems (Medcom)* pp. 34-337, 2014. *Crossref*, <https://doi.org/10.1109/MedCom.2014.7006028>
- [10] Abdul Rashid O. Mumin et al., "Square Ring Microstrip Patch Triple Band Antenna for GSM/ WIMAX/ WLAN Systems," *Proceeding International Conference on Control, Electronics, Renewable Energy and Communications ICCREC'2017*, pp. 70-74, 2017. *Crossref*, <https://doi.org/10.1109/ICCEREC.2017.8226675>
- [11] S. K. Sharma et al, "Triple Band Metamaterial Inspired Antenna Using FDTD Technique for WLAN/WIMAX Applications," *International Journal of RF and Microwave Computer-Aided Engineering*, vol. 25, no. 8, pp. 688–695, 2015. *Crossref*, <https://doi.org/10.1002/mmce.20907>
- [12] A. A. Deshmukh et al., "Triple Band E-Shaped Microstrip Antenna," *Procedia Computer Science*, vol. 93, pp. 67-73, 2016. *Crossref*, <https://doi.org/10.1016/j.procs.2016.07.183>
- [13] Liang Xu, Zhen-Yu Xin, and J. He, "A Compact Triple-Band Fork-Shaped Antenna for WLAN/WIMAX Applications," *Progress in Electromagnetics Research Letters*, vol. 40, pp. 61-69, 2013. *Crossref*, <http://dx.doi.org/10.2528/PIERL13040210>
- [14] Dhanraj Meena, and R. S. Meena, "Triple Band U-Slot Microstrip Patch Antenna for WLAN and Wireless Sensor Applications," *2015 Communication, Control and Intelligent Systems CCIS'2015*, pp. 12-14, 2015. *Crossref*, <https://doi.org/10.1109/CCIntelS.2015.7437866>
- [15] R. Ahmed, and Md. F. Islam, "W-Shaped Slot Microstrip Patch Antenna for Multiband Applications," *International Journal of Engineering Trends and Technology (IJETT)*, vol. 26, no. 5, pp. 282-285, 2015. *Crossref*, <http://dx.doi.org/10.14445/22315381/IJETT-V26P249>
- [16] Nilambar Muduli, and J.S.N Achary, "Analysis and Comparison of Liquid Sensing Using Silica and Bk7 Material Pcf By 2d Fdtd Method," *SSRG International Journal of Applied Physics*, vol. 5, no. 3, pp. 22-28, 2018. *Crossref*, <https://doi.org/10.14445/23500301/IJAP-V5I3P104>
- [17] Zh. Qian, Ru-S. Chen, K. Leung, and H. Yang, "FDTD Analysis of Microstrip Patch Antenna Covered by Plasma Sheath," *Progress in Electromagnetics Research, PIER*, vol. 52, pp. 173-183, 2005. *Crossref*, <http://dx.doi.org/10.2528/PIER04080901>
- [18] Eisuke Nishiyama et al, "FDTD Analysis of Stacked Microstrip Antenna With High Gain," *Progress in Electromagnetics Research, PIER*, vol. 33, pp. 29-43, 2001. *Crossref*, <http://dx.doi.org/10.2528/PIER00091501>
- [19] Y Ei. Hajibi, and A Ei. Hamichi, "Simulation and Numerical Modeling of a Rectangular Patch Antenna Using Finite Difference Time Domain (FDTD) Method," *Journal of Computer Science and Information Technology*, vol. 2, no. 2, pp. 01-08, 2014.
- [20] A. Boufrioua, E. Ksouri, and M. Harbadji, "Study By the FDTD Method of Multiband Microstrip Patch Antenna Loaded With L-Shaped Slot," *2019 IEEE/ACS 16th International Conference on Computer Systems and Applications (AICCSA)*, pp. 1-4, 2019. *Crossref*, <https://doi.org/10.1109/AICCSA47632.2019.9035334>
- [21] G. G. Bhide, A. B. Nandgaonkar, and S. L. Nalbalwar, "On the Novel Image Algorithms Filling Material Index Over the Finite-Difference Time-Domain Grid for Analysis of Microstrip Patch Antenna Using MATLAB," *Applied Computer Vision and Image Processing*, vol. 1155, pp.139-149, 2020. *Crossref*, http://dx.doi.org/10.1007/978-981-15-4029-5_14
- [22] G. Bhide et al., "Design and Analysis of Compact Giraffe-Shaped Patch Antenna for UWB Applications: A FDTD and Hybrid PSO Algorithm Approach," *International Journal of Engineering Trends and Technology*, vol. 70, no. 3, pp. 13-21, 2022. *Crossref*, <https://doi.org/10.14445/22315381/IJETT-V70I3P202>.
- [23] C.A. Balanis, *Antenna Theory: Analysis and Design*, 2nd Edition, John Wiley & Sons: New York, Usa, pp. 811-882, 2005.
- [24] A. Taflove, and S. C. Hagness, *Computational Electrodynamics: the Finite-Difference Time-Domain Method*, 3rd Edition Norwood Ma: Artech House, 2005.
- [25] A. Elsherbeni, and V. Demir, *The Finite-Difference Time-Domain Method for Electromagnetics With MATLAB Simulations*, 2nd Edition Raleigh, SciTech, 2016.
- [26] Matthew N.O. Sadiku, *Numerical Techniques in Electromagnetics*, 2nd Edition, CRC Press, 2001.
- [27] K. Sharmila and K. Kuppusamy, "An Efficient Image Compression Method Using Dct, Fractal and Run Length Encoding Techniques," *International Journal of Engineering Trends and Technology (IJETT)*, vol. 13, no. 6, pp. 287-290, 2014. *Crossref*, <https://doi.org/10.14445/22315381/IJETT-V13P257>
- [28] Sundara Rajan, P. V, and Fred, A. L, "An Efficient Compound Image Compression Using Optimal Discrete Wavelet Transform and Run Length Encoding Techniques," *Journal of Intelligent Systems*, vol. 28, no. 1, pp. 87–101, 2017. *Crossref*, <http://dx.doi.org/10.1515/jisys-2016-0096>
- [29] Kuang Fuqiang et al., "A Triple-Band Microstrip Antenna for WLAN Applications," *2010 International Conference on Communications and Mobile Computing, ICCMC'2010*, pp. 68-71, 2010. *Crossref*, <https://doi.org/10.1109/CMC.2010.66>
- [30] G. Bhide, A. Nandgaonkar, and S. Nalbalwar, "Dual-Band High Gain Union Shaped Micro-Strip Patch Antenna," *Proceedings of the International Conference on Communication and Signal Processing 2016 (ICCASP 2016)*, pp. 761-766, 2016. *Crossref*, <https://dx.doi.org/10.2991/iccasp-16.2017.106>